RSC Advances

ROYAL SOCIETY OF CHEMISTRY

www.rsc.org/advances

Diphenylether based derivatives as Fe (III) chemosensors: Spectrofluorimetry, Electrochemical and Theoretical studies

Rashmi Sharma, Manmohan Chhibber*, Susheel K Mittal
Thapar University, Patiala, India-147004.
E-mail:mchhibber@thapar.edu

Abstract

4-(2,4-dinitrophenoxy)-3-methoxybenzaldehyde (DPE-I) and (4-(2,4-dinitrophenoxy)-3-methoxyphenyl)methanol (DPE-II) were synthesized with high yield and characterized by spectroscopic techniques. The complexation behaviours of DPE-I and DPE-II for various cationic species (Na^+, K^+, Mg^{2+}, Cu^{2+}, Ba^{2+}, Cr^{3+}, Fe^{3+}, Co^{2+}, Ni^{2+}, Zn^{2+}, Cd^{2+}, and Pb^{2+}) in HEPES buffered CH_3CN: H_2O system were investigated and compared by spectroscopic and voltammetric techniques. Both receptors showed high degree of selectivity for Fe^{3+} over other cations. Receptors showed 1:1 complexation with Fe^{3+}. DPE-I showed fluorescence quenching on complexation with Fe^{3+} ion at 350nm due to PET (photon induced transfer) mechanism between Fe^{3+} and the large π electron conjugate system of ligand, while DPE-II displayed emission band at 314 nm which underwent fluorescence quenching selectively on gradual addition of Fe^{3+} at 314nm and simultaneously a new band at 424 nm emerged with isobestic point at 355 nm which increases with increase in Fe^{3+} conc. Electrochemically, DPE-I due to presence of electron withdrawing (aldehydic group) facilitates reduction of nitro group on benzene ring of the molecule so, peak potentials of the two curves obtained for DPE-I appear at -1.16 V (E_{pc1}) and -1.39 V (E_{pc2}) respectively, while in DPE-II (methanolic group) due to its electron donating character makes the reduction of nitro group a little difficult due to which peak potentials occur at higher potential as compared to DPE-I i.e. at -1.30 V (E_{pc1}) and -1.43 V(E_{pc2}) respectively.

Introduction

Synthesizing sensitive and selective chemosensor for specific metal detection is an interesting topic due to challenges in molecular design and their applications in a number of research fields [1–4]. Ionophores with functional groups like carboxylate [5,6], sulfonate [7,8], phosphonate [9–11], carbohydrate [12,13] and ammonium [14–16] can selectively trap metals ions. However, none of the attempts has been made to use diphenylether based

receptor having (R-O-R) ethereal linkage for metal detection. This is our first report using diphenylether based receptors for detection of iron.

Iron plays a significant role in many biochemical processes [17, 18] and is an important metal ion for most organisms. Fe^{3+} acts as a cofactor in many enzymatic reactions involved in the mitochondrial respiratory chain, and both its deficiency and excess can induce a variety of diseases [18–20]. A surplus of iron induces oxidative damage, rendering the intracellular scavenging of iron a major therapeutic target [21]. Therefore, methods of ferric ion detection have received a great deal of study. However, in spite of the important role of Fe^{3+} in chemical and biological processes, selective and sensitive chemosensors for Fe^{3+} are still rare.

In the past few years, several analytical techniques for the determination of trace amounts of Fe^{3+} have been reported, including atomic absorption spectrometry (AAS) [22], inductively coupled plasma-atomic emission spectrometry (ICP-AES) [23], inductively coupled plasma-mass spectrometry (ICP-MS) [24], electrochemical methods [25, 26] etc. Although these methods offer good limits of detection and wide linear ranges, most of these require the use of expensive and sophisticated instrumentation and complicated pretreatment procedures, not inappropriate for on-line or in-field monitoring. Owing to their advantages of simple equipment, rapid response, high sensitivity and easy operation, fluorescent approaches have been developed for the determination of Fe^{3+}. Currently, there have been a lot of developments in the field of Fe^{3+} chemosensors which have been used as fluorescent probes [27–41]. A comparative study of the chemosensors for Fe^{3+} has been shown in Table S1 [42, 7, 3, 43 and 44]. However, many of these probes exhibit either one or two of the following features that limit their practical applications. Firstly, most of the reported Fe^{3+} probes cannot work in aqueous media due to their hydrophobicity and low binding affinity. Secondly, most of these have interference problems caused by other transition metal cations such as Cu^{2+}, Co^{2+}, Al^{3+} or Hg^{2+}. Therefore, searching for highly selective chemosensors for Fe^{3+} in aqueous solutions is of great importance.

With purely organic hosts, appropriate geometry can sometimes be a problem for a proper host–guest interaction. On the other hand, metal ions can profitably orient the ligands in right conformations so that their hydrogen bond donor groups can converge towards an external guest. So, in this report, we have developed widespread diphenylether based chemosensors which get oriented in proper conformation to best fit the Fe^{3+} and hence can be used in various fields of analysis, as it can be used as a fluorescent chemosensor as well as

electrochemical chemosensor. In this manuscript, complexation behavior of **DPE-1** and **DPE-II** with various cations (Na^+, K^+, Cr^{3+}, Fe^{3+}, Co^{2+}, Ni^{2+}, Cu^{2+}, Zn^{2+}, Ba^{2+}, Hg^{2+},Cd^{2+} and Pb^{2+}) were investigated in aqueous media by spectrophotometric and voltammetric methods and the binding mode was further studied by using Gauss View 4.1.2 software.

Material and instrumental methods

Reagents and measurements

All reagents were purchased from commercial suppliers and used without further purification. Acetonitrile was distilled and was stored on molecular sieves before use. TLC analyses were performed on silica gel plates and column chromatography was conducted over silica gel (mesh 100–120). ^{1}H NMR spectra were recorded using JEOL A1 spectrometer operating at 400 MHz. ^{13}C NMR sepctra was recorded at 100 MHz. All chemical shifts are reported in ppm relative to the TMS as an internal reference. UV-Vis studies were carried out on a Analytic Jena machine using slit width of 1.0 cm and matched quartz cells. Fluorescence spectra were determined on a Perkin Elmer LS-55 fluorescence spectrometer.

Electrochemical measurements were carried out on Gamry Potentiostat/Galvanostat/ZRA Interface 1000. Solvents (acetonitrile, dichloromethane, dimethyl formamide) used in the spectrophotometric and electrochemical experiments were of HPLC grade (Sd Fine, India) and used as obtained. For cation interaction investigation, nitrate (Loba Chemie, India) and perchlorate salts (Sigma Aldrich) of the metal were used. Tetrabutylammonium hexaflouorophosphate (Sigma Aldrich) was used as a supporting electrolyte in all the voltammetric experiments. The working electrode was a glassy carbon electrode (CH Instruments, USA, 2 mm diameter). Platinum electrode was used as a counter electrode. All the potentials were reported against Ag/Ag^+ reference electrode. The Ag/Ag^+ electrode contained an internal solution of 0.01M $AgNO_3$ and 0.1M $TBAPF_6$ in solvents like acetonitrile, dimethyl formamide and dichloromethane. The working GC electrode was polished with alumina followed by washing with water and solvent before each cyclic voltammogram. The electrochemical measurements were carried out at a temperature of 25.0º ± 1º C. In all experiments, the test solutions were de-aerated by a stream of N_2 gas purging through the solution for at least 4-5 minutes.

Further, theoretical studies were performed by using Gauss View 4.1.2 software to know the binding mode of selective metal ion. For metal ion titrations, the solutions were prepared in

CH_3CN:H_2O (9:1, v/v) containing 10 mM HEPES buffer. Stock solution of DPE-I and DPE-II (10^{-3} M) were prepared in CH_3CN.

Synthesis

Compounds were synthesized as shown in Scheme 1 according to methods described in the literature [45]. Synthesized compounds were confirmed for their purity by melting point, TLC, ^1H and ^{13}C NMR spectroscopy which was in accordance with the previously reported literature (Figure S1 and S2).

Preparation of metal-ligand complexes

The binding ability studies of **DPE-I** and **DPE-II** were carried out with different metal ions viz. Na^+, K^+, Cr^{3+}, Fe^{3+}, Co^{2+}, Ni^{2+}, Cu^{2+}, Zn^{2+}, Ba^{2+}, Hg^{2+},Cd^{2+} and Pb^{2+} using spectroscopic and voltammetric experiments. **DPE-I** and **DPE-II** were taken in ACN: H_2O (9:1) medium. The solvent medium was prepared by taking 10mM of HEPES buffer to maintain pH = 7. Ligands **DPE-I** and **DPE-II** were taken in 20μM amounts to which 50 equivalents of each metal was added separately to prepare the metal-ligand complex solutions at 25 ºC. Those solutions of each metal with ligands were subjected to different studies on spectrophotometry, spectroflorimetry and voltammetry. Each study was conducted within 5 minutes of preparation of each metal-ligand complex.

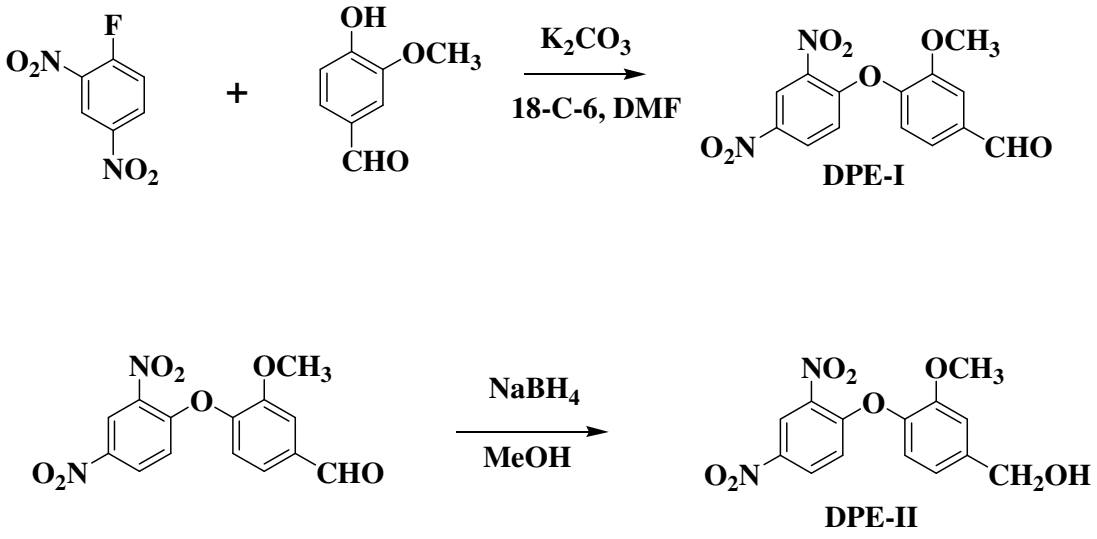

Scheme 1. Synthesis procedure of **DPE-I** and **DPE-II** compounds.

Results and discussion

UV-Vis studies

The UV-Vis spectroscopic studies of receptors DPE-I and DPE-II (20 μM) were investigated in HEPES buffered CH_3CN:H_2O (9:1; v/v) solvent system at pH 7.0 ± 0.1 because the pure CH_3CN solvent developed turbidity with receptors. DPE-I showed an absorption band at 240 nm while DPE-II showed an absorption band at 280 nm due to n→π* transition. On the addition of different metal ions, viz. Na^+, K^+, Cr^{3+}, Fe^{3+}, Co^{2+}, Ni^{2+}, Cu^{2+}, Zn^{2+}, Ba^{2+}, Hg^{2+},Cd^{2+} and Pb^{2+} to solutions of DPE-I and DPE-II, no significant changes in their respective UV-Vis spectra were observed except in the case of Fe^{3+} ions as shown in Figure S3. In order to evaluate the complete structural behaviour of DPE-I and DPE-II towards Fe^{3+}, titrations of DPE-I and DPE-II were performed with different concentrations of the metal ion. On the addition of 17 equivalents of Fe^{3+} to the solution of DPE I (Figure 1a), the absorption band at 240 nm gets flattened. A new band appears at 385 nm at 18 equivalents of Fe^{3+}. On further addition of iron solution there was an increase in absorption intensity at 385 nm which attains a saturation point after 46 equivalents. Similarly, for DPE-II, the absorption band at 280 nm gets flattened on the addition of 11 equivalents of Fe^{3+}, and a new band appears at 360 nm at 14.5 equivalents. On further addition of iron solution there was an increase in the absorption intensity of the band at 360 nm which attains a saturation point after 26.5 equivalents of Fe^{3+} as shown in Figure 1b. The absorption ratio at (240nm/385nm) two wavelengths varied from 0.03987 to 1.34262, indicating 33.67 fold absorption ratio changes for DPE-I while for DPE-II absorption ratio at two wavelengths (280nm/360nm) varied from 0.07597 to 0.96272, indicating 12.67 fold absorption ratio changes. Appearance of new bands at 385 nm and 360 nm, respectively for **DPE-I** and **DPE-II** on addition of Fe^{3+} (17 equivalents) indicate formation of the corresponding complexes. Further addition of Fe^{3+} ions resulting in increase in absorbance is due to the increase in concentration of the resulting metal-ligand complexes.

Thus, these chemo sensors can be used to estimate a wide range of Fe^{3+} ions ratio metrically between concentrations of 2×10^{-5} to 1×10^{-3} M and 2×10^{-5} to 6×10^{-4} M for DPE-I and DPE-II respectively, as shown in Figures 2a and 2b. The lower detection limit and stability constants for the complexes are shown in Table-1.

Table 1
Stability constants and some parameters of the **DPE –I** and **DPE-II** in the presence of Fe^{3+} in HEPES buffered $CH_3CN:H_20$ system

Complex	Coefficient of regression (R^2)	Stability constant	Detection limit
DPE-I+Fe^{3+}	0.999	$1.3 \times 10^3\ M^{-1}$	4.23×10^{-4} M
DPE-II+Fe^{3+}	0.998	$3.0 \times 10^3\ M^{-1}$	2.93×10^{-4} M

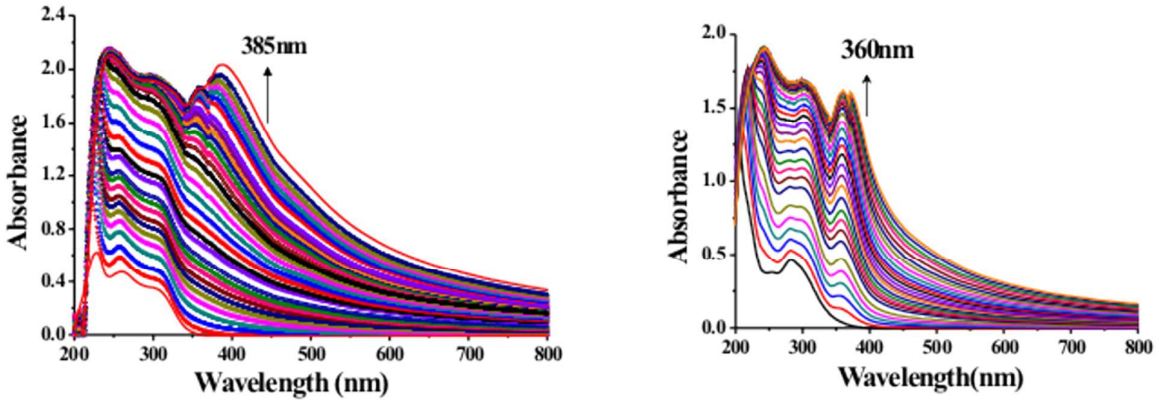

Figure 1 Absorption spectra of **(a) DPE- I** (20 µM) and **(b) DPE- II** (20 µM) at pH 7.0 ± 0.1 (10 mM HEPES in CH_3CN: H_2O 9: 1, v: v) upon complexation with increasing concentration of Fe^{3+} ions

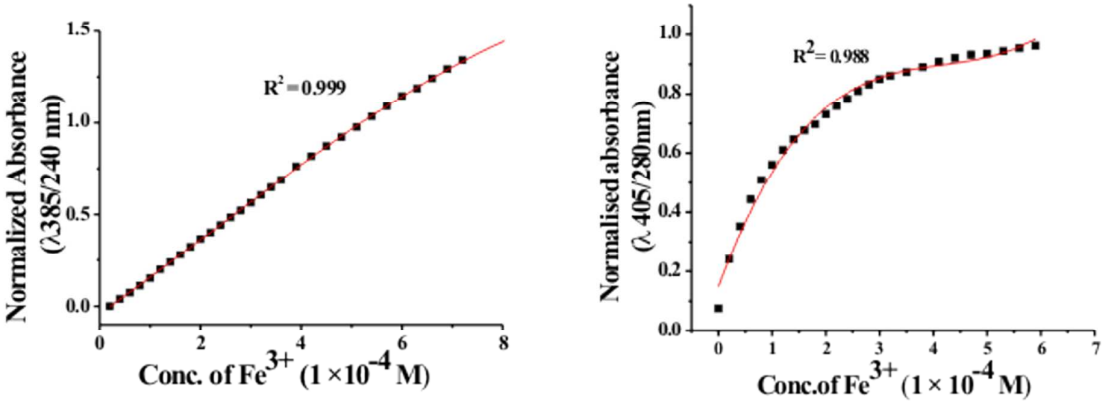

Figure 2 Ratiometric response of different concentrations of Fe^{3+} ions on **(a)** DPE-I (20 µM) and **(b)** DPE-II (20 µM) at pH 7.0 ± 0.1 (10 mM HEPES in CH_3CN: H_2O 9: 1, v: v).

To study practical applicability of DPE-I and DPE-II, competitive experiments were carried out in the presence of 10 equivalents of Fe^{3+} ions mixed with 50 equivalents of each of the different metal ions. No significant variations in the absorption spectra were observed in the

presence of a number of interfering metal ions like Na^+, K^+, Cr^{3+}, Fe^{3+}, Ni^{2+}, Cu^{2+}, Zn^{2+}, Ba^{2+}, and Pb^{2+}. Similar behaviour was observed for DPE-I and DPE-II compounds (Figure 3a, 3b).

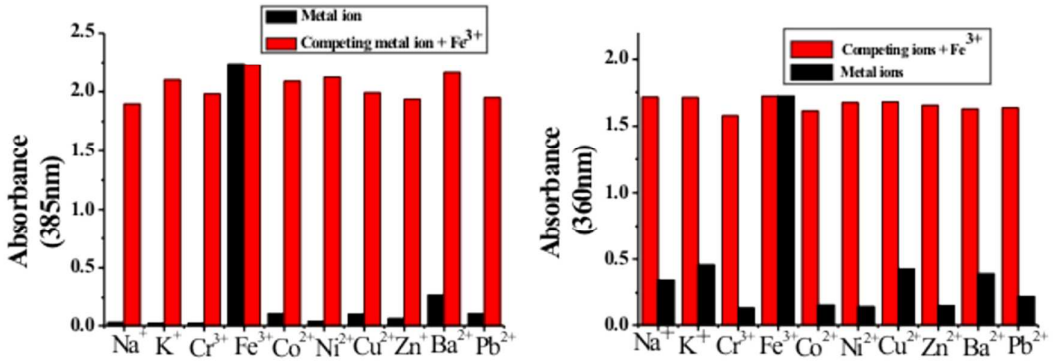

Figure 3 Black bars represent selectivity of (a) **DPE-I** and (b) **DPE-II** upon addition of different metal ions at pH 7.0 ± 0.1 (10 mM HEPES in CH_3CN: H_2O 9: 1, v: v) and red bars show the competitive selectivity of ligands in the presence of interfering metal ions

Emission properties of receptors

To obtain an insight into the fluorescent properties of the receptor, DPE-I was excited at 240 nm and displayed emission band at 350 nm. Further, complexation with different metal ions such as Na^+, K^+, Cr^{3+}, Fe^{3+}, Co^{2+}, Ni^{2+}, Cu^{2+}, Zn^{2+}, Ba^{2+}, Hg^{2+},Cd^{2+} and Pb^{2+} in CH_3CN: H_20 (9:1, v/v) were studied, which underwent fluorescence quenching selectively on addition of Fe^{3+}, whereas other metal ions did not show any significant change. While DPE-II was excited at 280 nm which displayed emission band at 314 nm which underwent fluorescence quenching selectively on gradual addition of Fe^{3+}. Simultaneous to the quenching process a new band at 424 nm emerged with isobestic point at 355 nm. The emission at 424 nm increases with increase in Fe^{3+} conc., whereas other metal ions did not show any significant change. In order to evaluate the complete structural behaviour of DPE-I and DPE-II towards Fe^{3+}, the fluorescence titrations of DPE-I and DPE-II were performed at different concentrations of metal ions as shown in Figure 4a and 4b.

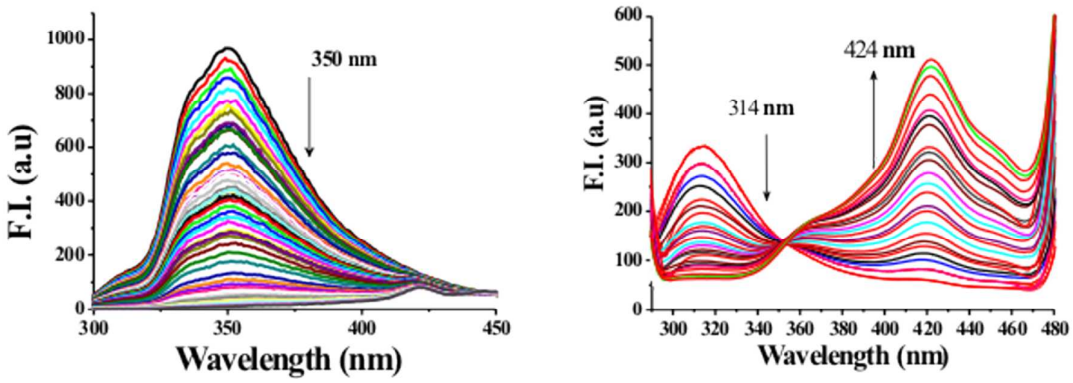

Figure 4 (a) Fluorescence spectra of (a) **DPE-I** and **(b) DPE-II** (20 μM) at pH 7.0 ± 0.1 (10 mM HEPES in CH_3CN: H_2O 9: 1, v: v), upon complexation with increasing concentration of Fe^{3+} ions

Ratiometric behaviour of DPE-I and DPE-II in presence of different Fe^{3+} concentrations is shown in Figure S4. In the fluorescence titration of DPE I with Fe^{3+} ions, the plot of I_o/ I (I_0 and I, fluorescence intensity of DPE I without and with Fe^{3+} ions) vs. Fe (III) concentration was not a straight line. This indicated that the fluorescence quenching of DPE I by Fe^{3+} ions did not obey the Stern–Volmer quenching equation ($I_0/I = 1 + K$ [Fe]). Therefore, the fluorescence quenching is a static quenching. The disappearance in fluorescence intensity of DPE-I on interaction with Fe^{3+} may be explained by the favourable photo induced electron transfer (PET) mechanism between ligand and Fe^{3+} [46] while such mechanism was not supported for DPE-II. PET mechanism is observed in DPE-I as the lone pairs on oxygen of –CHO are engaged through conjugation with Fe^{3+}. In case of DPE-II, the lone pairs on oxygen of –OH not being conjugated with the benzene ring are available for excitation resulting in emission band at 424 nm and no PET mechanism is observed.

The linear ratiometric response (I_{424}/I_{314}) in case of DPE-II, with increasing concentration of Fe^{3+} also makes it a unique probe for it. Presence of isobestic point at 355 nm proves that one intermediate is formed before complete complexation which is also highly fluorescent and fluorescent intensity at 424 nm goes on increasing upto 50 equivalents of Fe^{3+} ions due to complex formed between DPE-II and Fe^{3+}. The Fe^{3+} ions are likely to bind to the ligands via O-atoms of the nitro and methoxy groups. The PET process occurs due to the transfer of electron density from ligand to the metal ion. The higher the charge density a cation possesses (the charge density of Fe^{3+} is 6.09) [47], the stronger the electronic affinity it provides. So, it is reasonable to be used to achieve PET processes between Fe^{3+} and the large π electron conjugate system of ligand. Moreover, from theoretical studies it is observed that the DPE-I is a good electron donor, which displays an ability to coordinate Fe^{3+} ions, so that there can be a reasonable charge transfer between DPE-I and the Fe^{3+} ions.

The non-linear regression analysis of fluorescence data for Fe-DPE I complex showed the formation of 1:1 complex with association constant 5.1×10^3 M^{-1} while DPE-II showed better association constant of 7×10^3 M^{-1}. To elicit the interactions between Fe^{3+} and DPE-I and DPE-II respectively, the binding stoichiometry was determined by the Job's plot [48, 49]. The Job's function F_{Job} is calculated according to the equation $F_{Job} = (1 - X) F_0 - F$. The plot

of the fluorescence versus the mole fraction of the added Fe^{3+} (Figures 5a and 5b,) shows two parts that can be fitted by straight lines. The lines intersect at X equal to 0.5. These results reveal the formation of a 1:1 complex formulated as DPE-I $–Fe^{3+}$ and DPE-II $–Fe^{3+}$, respectively.

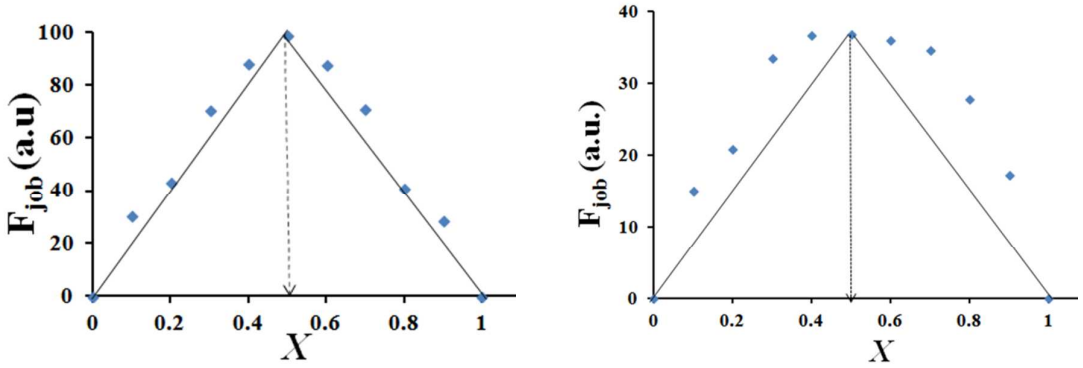

Figure 5 Job's plot of (a) **DPE-I** and Fe^{3+} (b) **DPE-II** and Fe^{3+} which indicated the stoichiometry of **L**-Fe^{3+} complex is 1:1

Electrochemical measurements

Electrochemical properties of **DPE-I** and **DPE-II** were investigated by CV and DPV. The cyclic voltammograms for **DPE-I** and **DPE-II** in CH_3CN:H_2O (9:1, v/v) solution containing 0.1 M $TBAPF_6$ as the supporting electrolyte are shown in **Figures 6a and 6b**.

Electrochemical behaviour of DPE-I and DPE-II

Synthesis of DPE-I and DPE-II containing electron donating and electron withdrawing substituents, respectively was done to check their remote substituent effect on the electronic environment around the ethereal oxygen of the diphenylether group. These compounds are identified as DPE-I (containing –CHO group meta to methoxy group on benzene ring) and DPE-II (containing $–CH_2OH$ group meta to methoxy group on benzene ring). It is hypothicated that the aldehydic group should facilitate reduction of nitro group on benzene ring of the molecule, while methanolic group, due to its electron donating character, should make the reduction of nitro group, a little difficult. Peak potentials of the two curves obtained for DPE-I appear at -1.16 V (E_{pc1}) and -1.39 V (E_{pc2}), respectively, whereas corresponding peaks for DPE-II are observed at -1.30 V (E_{pc1}) and -1.43 V(E_{pc2}), respectively (Figures 6a and 6b). Corresponding peak currents for the respective peak potentials are shown in Table 2.

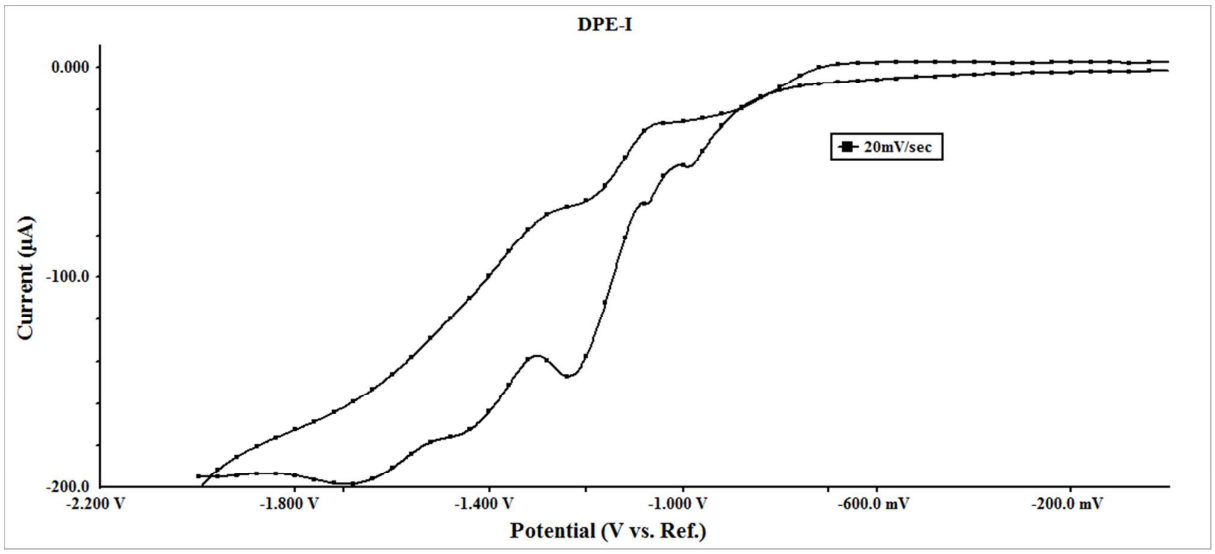

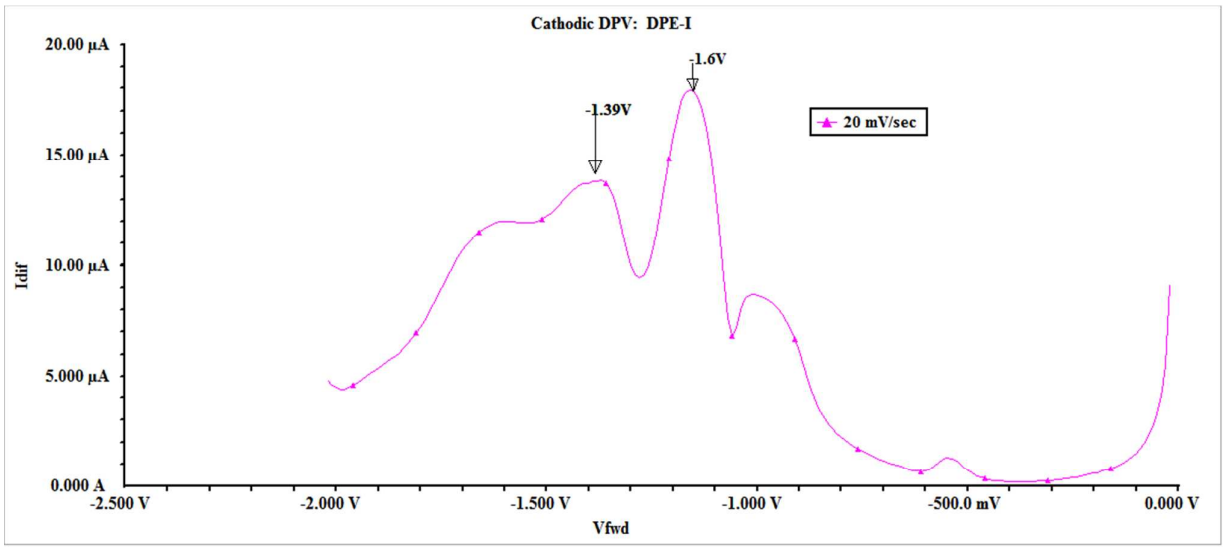

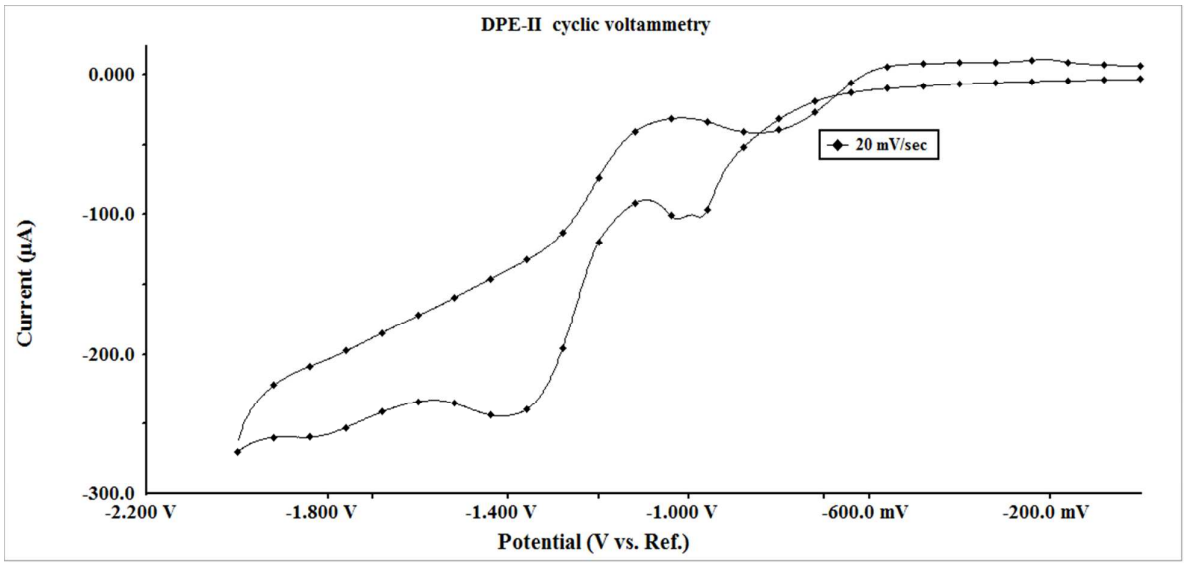

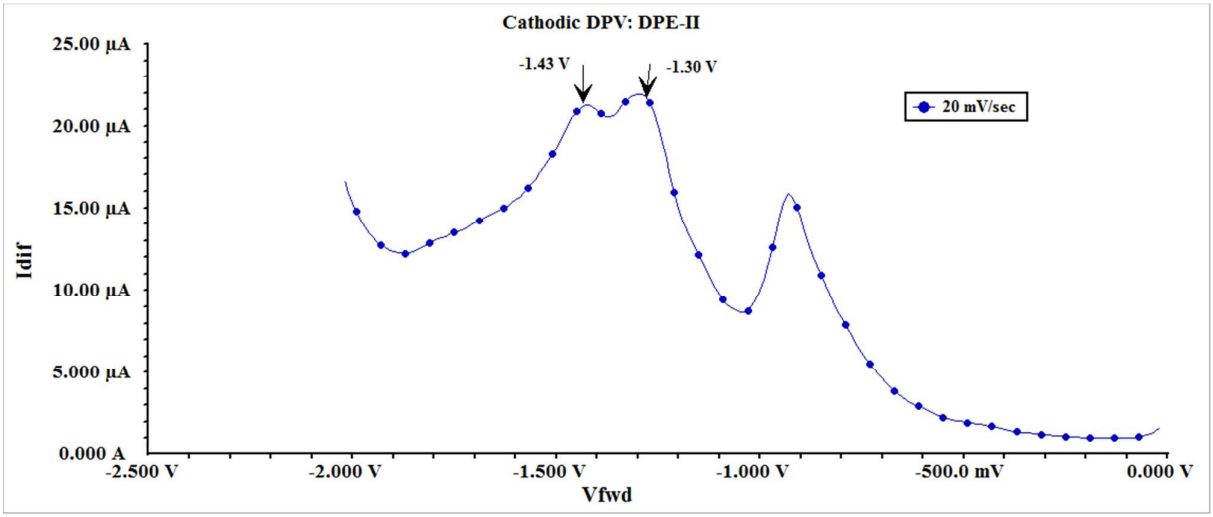

Figure 6 Cyclic and differential pulse voltammograms of (a) **DPE-I** (b) **DPE-II** (5×10^{-4}M) at pH 7.0 ± 0.1 (10 mM HEPES in CH_3CN : H_2O 9 : 1, v : v) using 0.1M $TBAPF_6$ as supporting electrolyte, scan rate 20 mV s^{-1} and GC as working electrode. Modulation amplitude for DPV: 50mVsec^{-1}

Table 2 Peak potential (V) and peak current (µA) values for **DPE-I** and **DPE-II** (5×10^{-4}M), scan rate 100mV/sec

Compound	**Peak potentials (V)**		**Cathodic peak currents (µA)**	
	$E_{pc}1$	$E_{pc}2$	$i_{pc}1$	$i_{pc}2$
DPE-I	-1.16	-1.39	-45.7	-37.4
DPE-II	-1.30	-1.43	-62.6	-76.5

Effect of scan rate

In order to understand nature of the electrode processes taking place for DPE-I and DPE-II, peak currents of cathodic waves were plotted against square root of scan rate (Figure 7). A linear relation between peak current and square root of scan rate shows that Fick's law of diffusion is obeyed and the charge transport is diffusion based process. For DPE-II with increase in scan rate from 20 mV s^{-1} to 100 mV s^{-1}, two separate reduction peaks at -1.30 V and -1.43 V merge to form a single broad reduction peak. It indicated that at higher scan rates the two different reduction processes were observed as a single step, while for DPE-I both the

reduction steps were observed as separate peaks even at 200 mV s^{-1} or higher scan rates. This observation is also supported by the DPV curves (Figure S5).

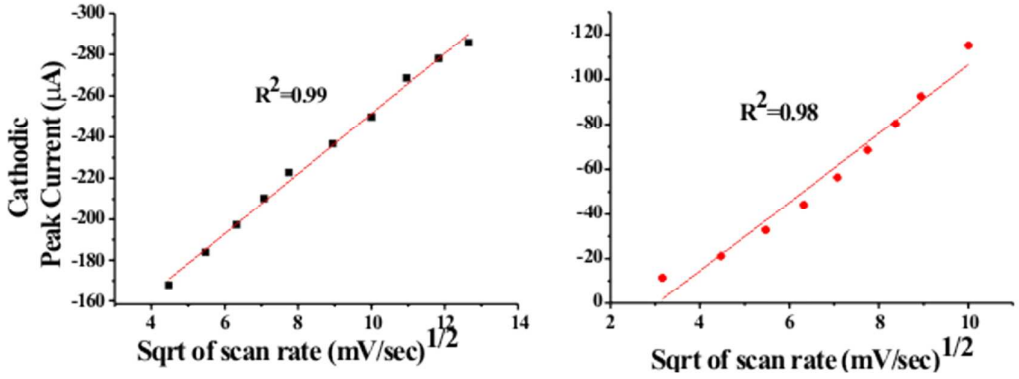

Figure 7 Plots of peak current and square root of scan rate for **DPE-I** and **DPE-II**

Effect of concentration of the electroactive compound

Electrochemical study of the compounds DPE-I and DPE-II was done to know the effect of different concentrations on their respective CV behaviors. Results are shown in Figure S6. With increase in concentration of each of DPE-I and DPE-II, a corresponding increase in the respective peak currents was observed along with a cathodic shift in the peak potential. This is due to the reason that increase in concentration of redox substances makes the velocity of mass diffusion rapid and hence the electrode processes become more controlled by the electrode reactions. Calibrations for concentration of analyte species and cathodic peak currents were plotted and observed coefficients of regression varied within range 0.98-0.99, as shown in Figure 8.

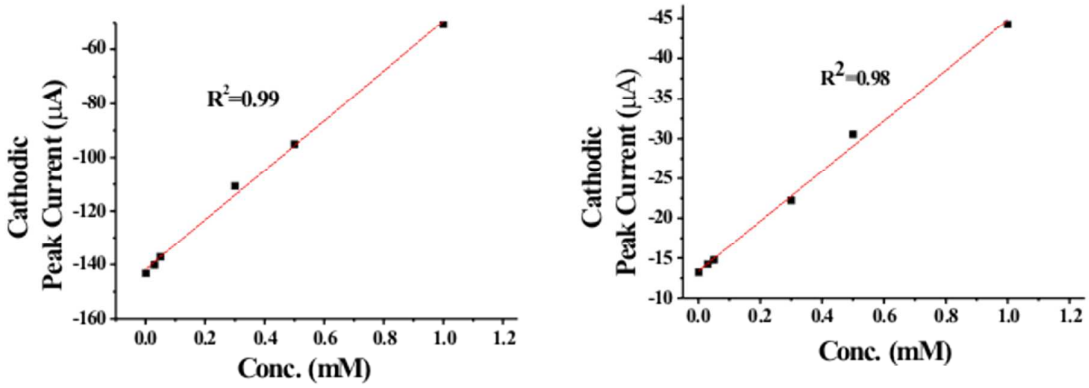

Figure 8 Calibration curves between concentrations of receptors and peak current for **DPE-I** and **DPE-II**

Effect of solvent

Receptors DPE-I and DPE-II were studied for their voltammetry in different solvent systems like dicholormethane (DCM), acetonitrile (ACN) and N, N-dimethylforamide (DMF). In addition, mixed solvent systems of ACN: H_20 (9:1, v/v) and DMF: H_20 (9:1, v/v) were also taken for the study anticipating some interactions of water with substituents –CHO in DPE-I and $–CH_2OH$ in DPE-II. Cyclic voltammetric and differential pulse voltammetric graphs for DPE-I and DPE-II in different solvent media are shown in Figure S7.

DPV peaks for both the compounds in all solvent systems are identified in Table 3. It is interesting to note that DPE-I shows only one reduction peak while DPE-II shows three reduction peaks in ACN solvent system. These can be explained as below:

In receptor DPE-I there are three prominent functional groups like –CHO, $-OCH_3$ and $–NO_2$ which can be responsible for the cathodic current peaks. Amongst these three groups, because of its electron withdrawing inductive effect nitro is the most probable candidate for reduction and hence shows a peak at lowest value of applied potential i.e. -1.36V. The absence of peaks in DPE-I (-1.68V) and DPE-II (-1.85V) is due to replacement of carbonyl bearing functional group –CHO in DPE-I with $–CH_2OH$ in DPE-II. This change in functional group infact easies out electron withdrawing tendency of ethereal oxygen para to –CHO group, hence the absence of cathodic peak at -1.68V. The cathodic peak at -1.68V in DPE-II is probably due to methoxy group as the peak at -1.85V in DPE-II disappears with change in solvent system from ACN to ACN: H_2O (9:1, v/v) system due to interaction of $-OCH_3$ group indicating its involvement with H_2O through hydrogen bonding. Moreover, the absence of corresponding peak (-1.85V) in DPE-I in both ACN and its mixture with water can also be justified due to poor reduction potential of –CHO (in DPE-I) as compared to $–CH_2OH$ (in DPE-II). The

absence of E_{pc3} in ACN: H_2O solvent system is clear indication of hydrogen bonding of CH_2OH group with water as shown below:

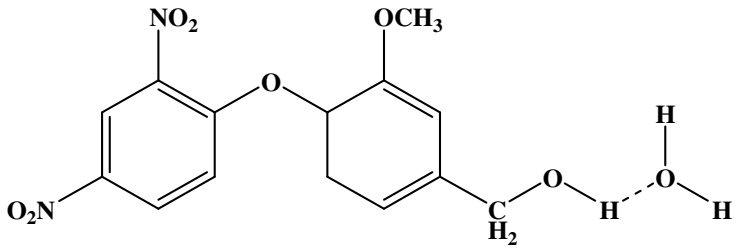

Hydrogen bonding of -CH_2OH group of DPE-II with water molecule

In solvent media like DCM, the main observation as compared with ACN solvent system is with regard to shift in all peaks of DPE-I and DPE-II to lower potential values. This important shift is due to low dipole moment of DCM (1.60 D) as compared to ACN (3.92 D) and DMF (3.86 D). Hence, polarity of the solvent does influence reduction potentials of target molecules. It is further noticed that the reduction potentials of DPE-I and DPE-II are almost similar due to similar dipole moments of ACN and DMF solvents.

Table 3 Peak potentials (V) for **DPE-I** and **DPE-II** (5×10^{-4}M) in different solvent systems

Solvent	Dipole moment (D)	DPE-I			DPE-II		
		E_{pc1} (V)	E_{pc2} (V)	E_{pc3} (V)	E_{pc1} (V)	E_{pc2} (V)	E_{pc3} (V)
ACN	3.92	-1.36	-----	----	-1.32	-1.68	-1.85
DMF	3.86	-1.25	-1.48	-1.87	-1.348,	-1.70	-1.89
DCM	1.60	-1.23	-1.47	-1.750	-1.290	-1.62	-1.82
ACN:H_20		-1.16	-1.39	----	-1.30	-1.43	----

Metal-Ligand complexation studies

Voltammetric studies of the synthesized diphenylether based compounds were performed to study their tendency to complex with transition metal ions so that these can be projected as ionophores suitable for heavy metal detection by simple voltammetric methods. DPE-I and DPE-II were studied for their tendency for complexation with Fe^{3+} ions. Voltammograms were drawn for both DPE-I and DPE-II with and without Fe^{3+} ions. Significant decrease in current magnitude of E_{p1} and E_{p2} from 45.7 µA to 9.7 µA and 37.4 µA to 11.0 µA respectively, for DPE-I prompted us to study complexation on a quantitative way as shown in Figure 9. Incremental amounts of Fe^{3+} were added to 2.5 µmoles of DPE-I and the resulting current magnitude are given in Table 4. Similar experiments were carried out on DPE-II compound. It can be seen from Table 3 that with addition of increasing concentration of Fe^{3+}, a linear fall in cathodic peak current is observed till metal ions ratio with the ligand is reached 1:1 (Figure 10). Further addition of the metal ions did not bring any further change in current magnitude. Exactly similar trend in current magnitude was observed for DPE-II. Hence, DPE-I and DPE-II can be projected as ionophores for Fe^{3+} metal detection. Calibration curves for the detection of Fe^{3+} using DPE-I and DPE-II are shown in Figure 10. The proposed method is valid for the detection of Fe^{3+} species in the concentration range 0-2.5 µmoles. Presence of other metal ions (Na^{+}, K^{+}, Cr^{3+}, Fe^{3+}, Co^{2+}, Ni^{2+}, Cu^{2+}, Zn^{2+}, Ba^{2+}, Hg^{2+},Cd^{2+} and Pb^{2+}) have also been studied and results indicate selectivity for Fe^{3+} ions only.

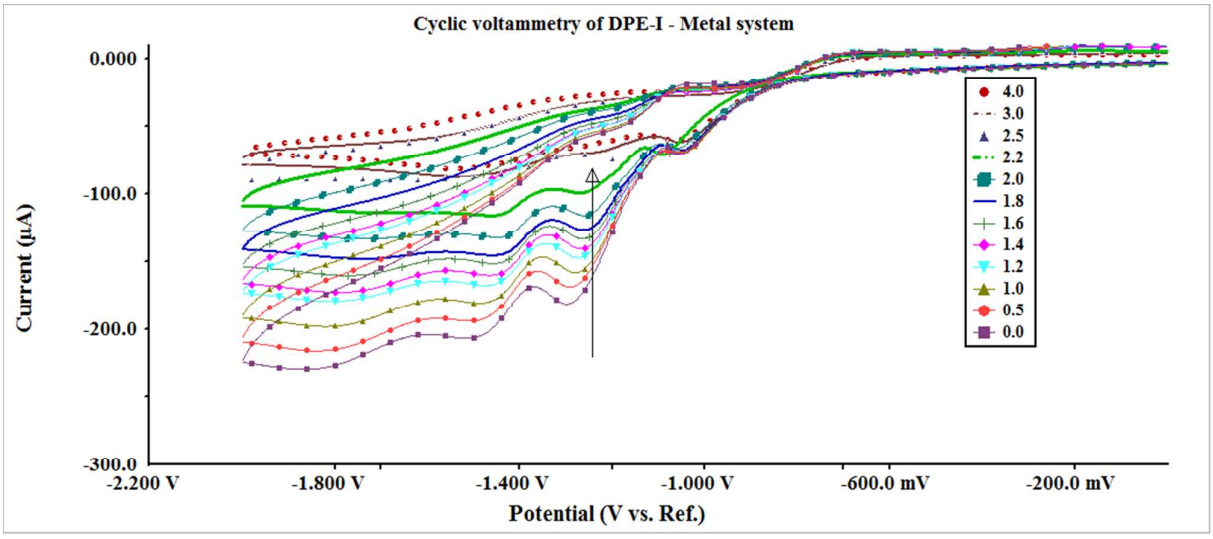

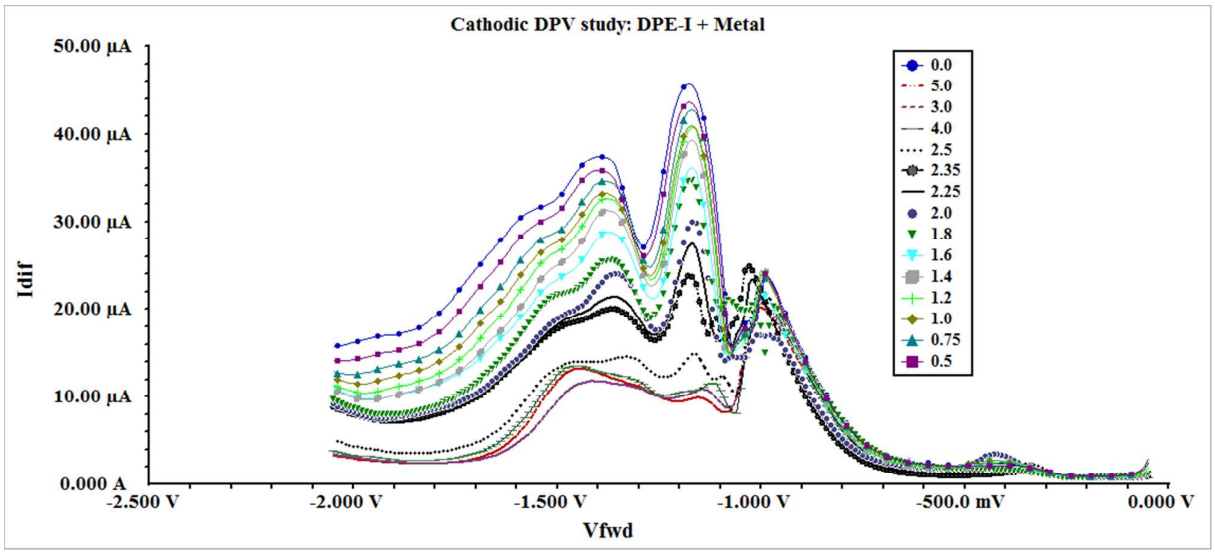

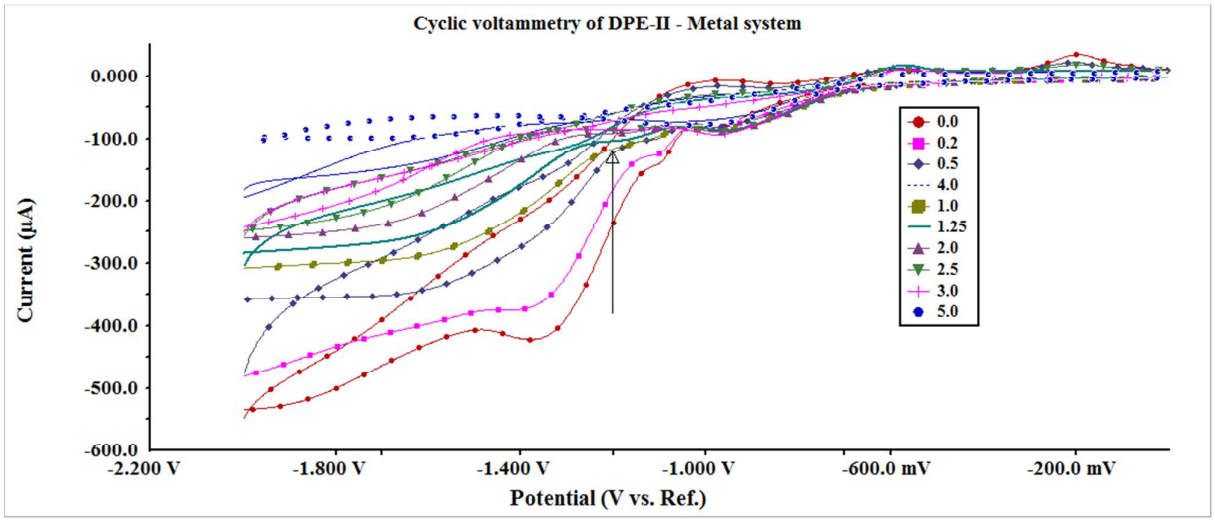

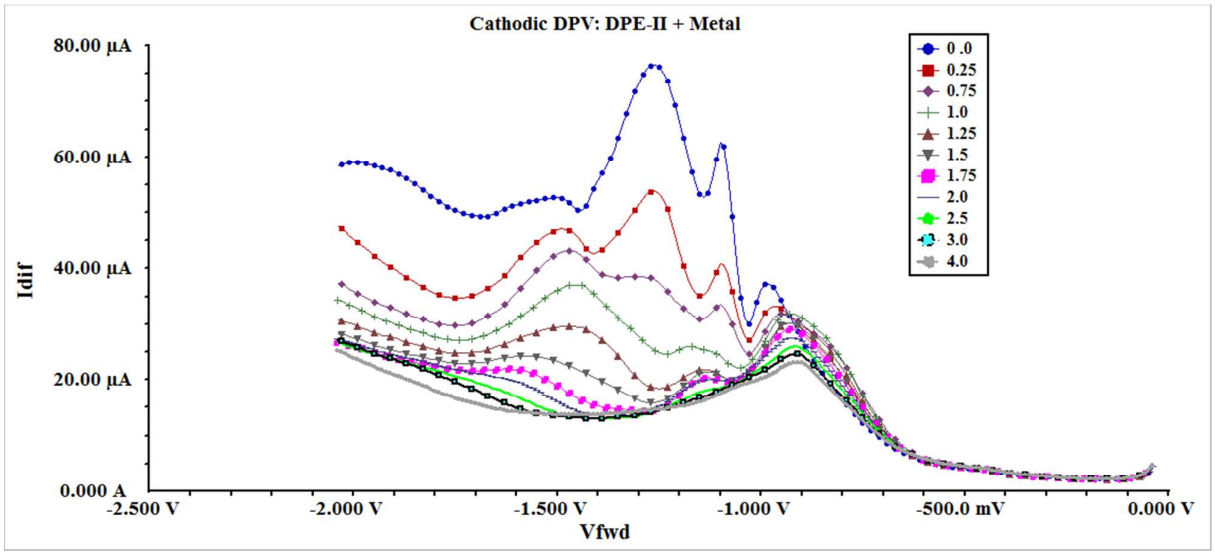

Figure 9 Cyclic and differential pulse voltammaograms of Ligands (DPE-I and DPE-II) upon increment addition of metal (μM Fe^{3+}) at pH 7.0 ± 0.1 (10 mM HEPES in CH_3CN: H_2O 9: 1, v: v), 0.1M $TBAPF_6$

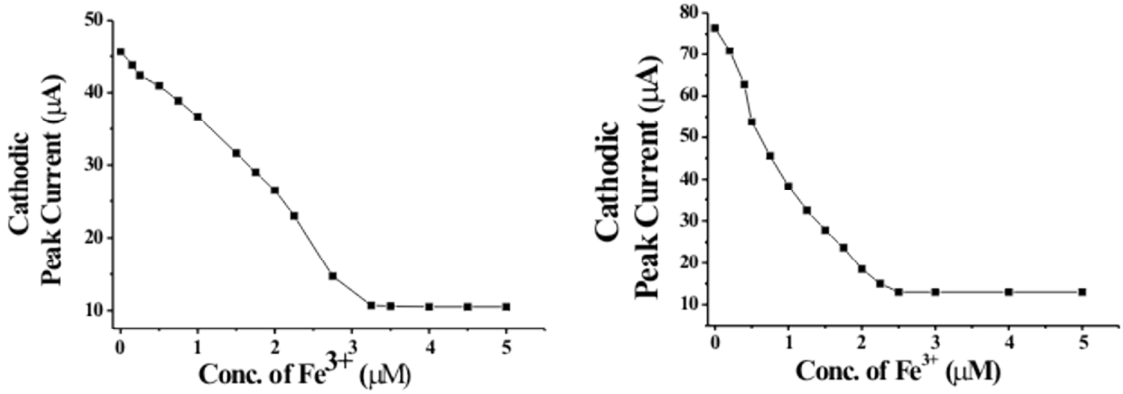

Figure 10 Calibration curves showing response of metal (Fe^{3+}) addition to ligands (a) **DPE-I** and (b) **DPE-II**

Table 4 Peak current values for **DPE-I** and **DPE-II** with and without Fe^{3+} ion

Ligand 'L' (DPE-I /DPE-II)	**DPE-I**				**DPE-II**			
	i_{p2} (-1.39V) μA	**i_{p1} (-1.16V) μA**	**Δi_{p2} (-1.39V) μA**	**Δi_{p1} (-1.16V) μA**	**i_{p2} (-1.43V) μA**	**i_{p1} (-1.30V) μA**	**Δi_{p2} (-1.43V) μA**	**Δi_{p1} (-1.30V) μA**
Without metal (2.5μmoles)	-37.43	-45.67	---	---	-76.51	-62.59	---	---
L +Fe^{3+} (0.5μmoles)	-32.64	-40.79	-4.79	-4.88	-53.79	-40.82	-22.72	-21.77
L +Fe^{3+} (1.0μmoles)	-24.08	-30.01	-13.35	-15.66	-38.29	-33.56	-38.22	-29.03
L +Fe^{3+} (1.5μmoles)	-20.05	-23.75	-17.38	-21.92	-27.77	-24.61	-48.74	-37.98
L +Fe^{3+} (2.5μmoles)	-14.56	-14.85	-22.87	-31.07	-13.03	-15.99	-63.48	-46.60
L +Fe^{3+} (2.8μmoles)	-11.01	-10.71	-26.42	-34.96	-13.02	-15.90	-63.49	-46.69
L +Fe^{3+} (3.5μmoles)	-11.01	-9.73	-26.42	-35.94	-13.02	-15.90	-63.49	-46.69

Interference studies

Selectivity of DPE-I and DPE-II was confirmed further by interference studies with various interfering metal ions added in excess to the target metal ion. Voltammetric study was done to study the effect of the presence of other ions on the response of DPE-I and DPE-II for Fe^{3+} ions. Both the derivatives responded selectively to Fe^{3+} ions even in the presence of other metal ions (Table 5) as indicated from the quenching of the electroactive nature of ligands (DPE-I and DPE-II) i.e. large decrease in peak currents. After complexation with the metal ions, the receptors donot remain electroactive due to non-availability of lone pair of electrons on the heteroatoms.

Table 5 Peak potential (V) values for **DPE-I** and **DPE-II** alone and with different metal ions

Metal studied	**DPE-I**		**DPE-II**	
	E_{p1} (V)	E_{p2} (V)	E_{p1} (V)	E_{p2} (V)
Ligand	-1.16	-1.39	-1.30	-1.43
Na^{+}	-1.20	-1.36	-1.31	-1.45
K^{+}	-1.14	-1.38	-1.23	-1.41
Mg^{2+}	-1.15	-1.39	-1.27	-1.41
Cr^{3+}	-1.01	-1.22	-1.21	-1.42
Fe^{3+}	--	--	--	--
Co^{2+}	-1.14	-1.36	-1.30	-1.42
Cu^{2+}	-1.16	-1.36	-1.28	-1.42
Zn^{2+}	-1.10	-1.35	-1.32	-1.44
Ba^{2+}	-1.16	-1.39	-1.29	-1.38

Theoretical Studies

The computational study was carried out by using Density Functional Theory (DFT) in an attempt to better understand the nature of receptors and their interaction with metal ion. The B3LYP function was employed for calculations with 6-31G basis set on Gaussian 03W programmer except for Fe^{3+}, for which LanL2DZ was used [50-53]. The receptors DPE-1 and DPE-II have three dimensional structure forming a pseudo cavity between ethereal oxygen, nitrogen of nitro group and oxygen of methoxy group and B3LYP/6-31G basis set was employed for their optimization (Figure 11a, 11b). However, DPE I-Fe^{3+} and DPE II-Fe^{3+} were optimized by using B3LYP/6-31G and LanL2DZ basis set for Fe^{3+} (Figure 11c, 11d).

Optimized structures revealed the possible mode of complexation in which ether group, due to its flexible nature gets rotated and forms best fit metal-ligand coordination sites between Fe^{3+} and the receptors. On coordination with Fe^{3+}, there is an increase in the stability of the

whole system which was confirmed from the value of energy optimization (Table 6). The gap between HOMO-LUMO is less for DPE I-Fe^{3+} and DPE II-Fe^{3+} as compared to receptor DPE-1 and DPE-II alone, as depicted in Figure 12. Further, the HOMO-LUMO of the DPE-I+Fe^{3+} and DPE-II+Fe^{3+} showed that LUMO is main contributor in electronic transition [50, 51].

Binding energies obtained from theoretical studies (as shown in Table S2) have proved that energy values of DPE molecules decrease with the addition of Fe^{3+}. Energy for DPE-I decreases from -1175 a.u to -1298 a.u while for DPE-II energy decrease found was from -1177 a.u to -1299 a.u. Hence, leading to the formation of the stable complexes. Energy decrease in case of DPE-II is slightly more than that of DPE-I proving DPE-II to be more stable than DPE-I.

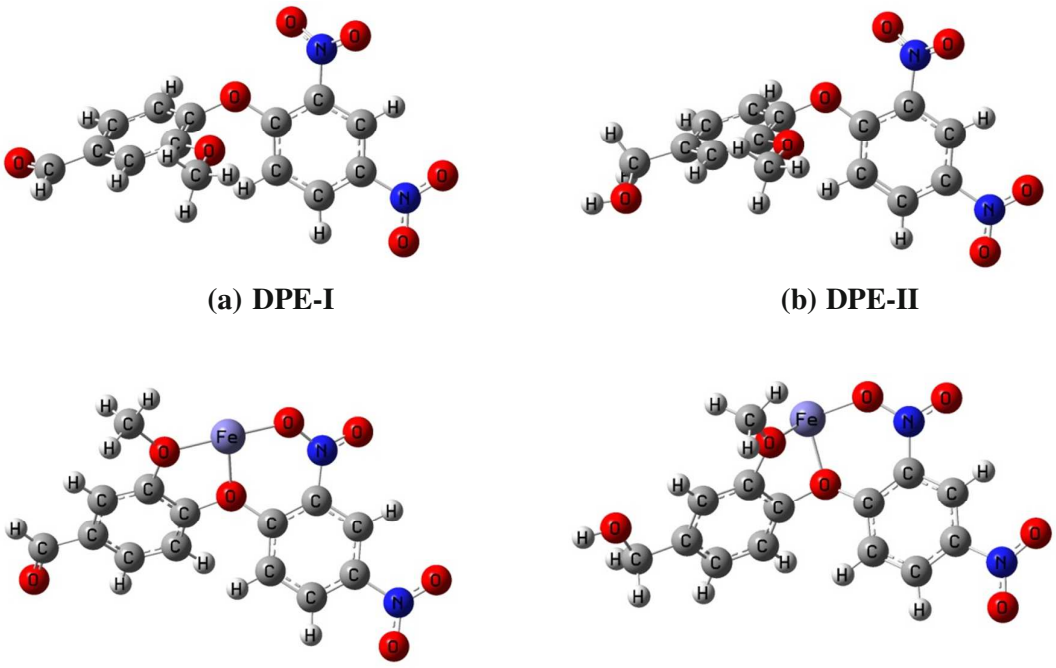

(a) DPE-I **(b) DPE-II**

(c) DPE-I+Fe^{3+} **(d) DPE-II+Fe^{3+}**

Figure 11 The DFT optimized structures of receptors **DPE-I** and **DPE-II** and their complexes with **Fe^{3+}**calculated at the B3LYP/6-31G/LanL2DZ level respectively. The red, blue, gray, and purple spheres refer to O, N, C, and Fe, respectively

Table 6 Energy values (in a.u) of HOMO, LUMO and LUMO+1 for **DPE-I** and **DPE-II** and their complexes with **Fe^{3+}**

Receptor	Energy in a.u				
	E_{HOMO}	E_{LUMO}	E_{LUMO+1}	E_{gap1}	E_{gap2}
DPE-I	0.256	0.113	0.107	0.143	0.149
DPE-I+Fe^{3+}	0.487	0.468	0.435	0.019	0.052
DPE-II	0.236	0.093	0.087	0.143	0.149
DPE-II+Fe^{3+}	0.488	0.467	0.453	0.021	0.035

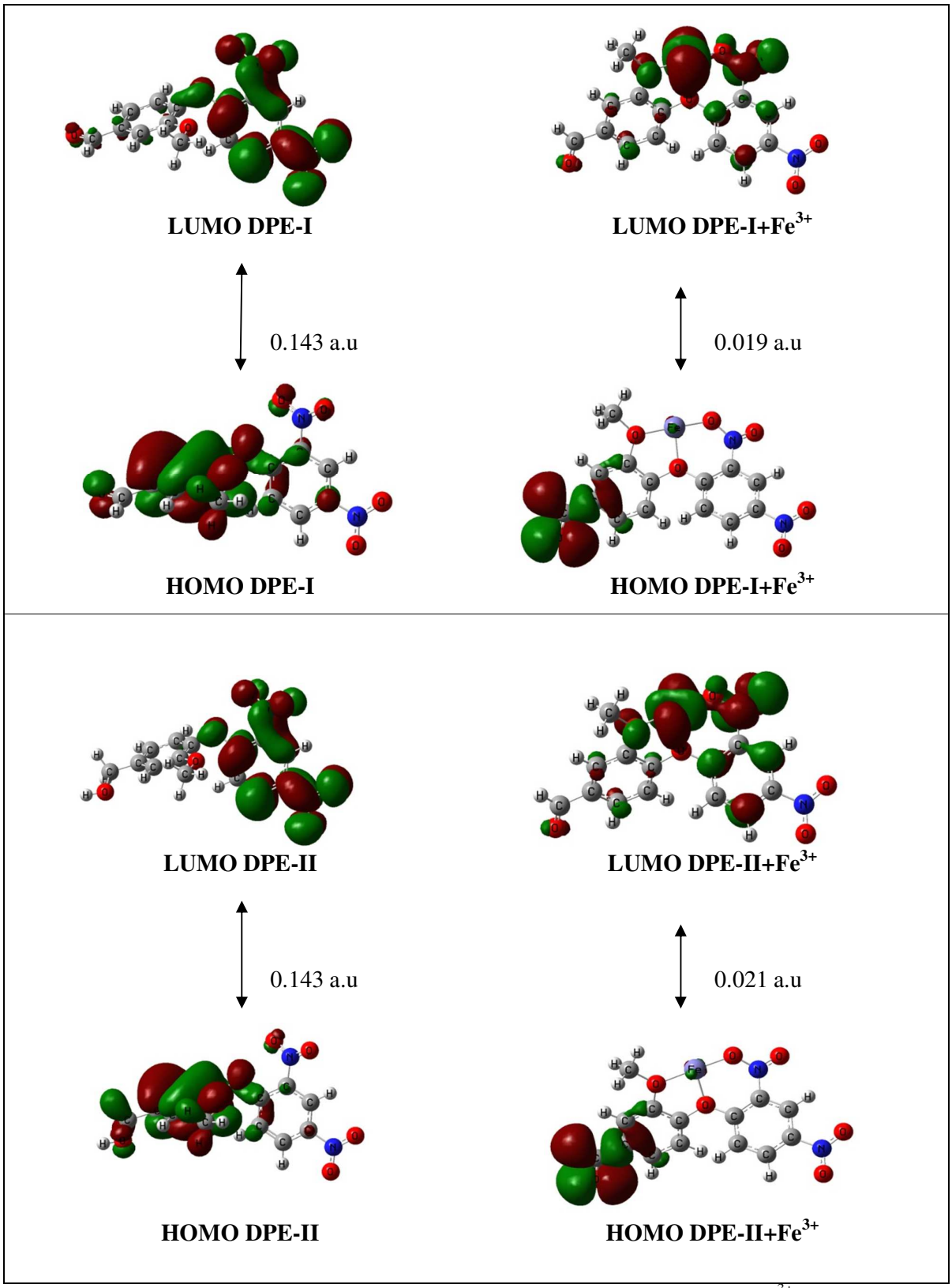

Figure 12 The HOMO-LUMO gap of: receptors DPE-I and DPE-II and their Fe^{3+} complexes calculated at the B3LYP/6-31G/LANL2DZ level respectively.

Real Life sampling

In order to test the analytical applicability of the proposed voltammetric method, the chemosensors were used for the determination of iron in pharmaceutical samples (Feriron) and water samples (tap water and mineral water) and some synthetic samples.

Pharmaceutical sample was prepared by dissolving one tablet of Feriron in 10 mL HCl and heated to dryness. After that, the sample was dissolved in 10 mL distillated water, filtered and transferred to a 25 mL standard flask and this volume was completed with distillated water. Each synthetic sample was spiked with the addition of 1 mL of 10^{-2} M standard metal ion solution, keeping the total volume of the sample equal to 100 mL. Complexometric method was also used for the determination of iron contents in these samples. The results of the voltammetric sensors obtained are presented in Table 7 and compared with those obtained by using complexation with EDTA. The sensors are found to be in satisfactory agreement with those obtained from the complexometric method. These observations and results have confirmed that present chemosensors can be used for practical analysis.

Table 7 Determination of Fe (III) in real samples using complexometric method and proposed chemosensors

Sample Name	Adjusted pH	Total Iron Found ($\mu g \cdot ml^{-1}$ or $g \cdot kg^{-1}$)			
		Chemosensor (**DPE-1**)	Complexometric method	Chemosensor (**DPE-II**)	Complexometric method
Feriron	3.5	10.7 ± 0.02	11.1 ± 0.03	12.5 ± 0.02	12.2 ± 0.01
Tap Water	3.5	6.1 ± 0.08	6.4 ± 0.06	6.59 ± 0.07	7.1 ± 0.02
Mineral Water	3.5	5.3 ± 0.01	5.1 ± 0.01	4.89 ± 0.06	4.9 ± 0.02
RS-1	3.5	11.53 ± 0.03	11.4 ± 0.03	12.79 ± 0.05	12.7 ± 0.01
RS-2	3.5	15.39 ± 0.02	15.5 ± 0.04	16.89 ± 0.05	16.9 ± 0.04

± Shows the standard deviation (n=3).

Acknowledgments

We thank BRNS, BARC Mumbai for financial assistance vide research grant no. 2012/37C/5/BRNS/621 and we also thank SAI Labs, Thapar University, Patiala for NMR studies.

References

1. G. W. Gokel, W. M. Leevy and M. E. Weber, *Chemical Reviews*, 2004, **104**, 2723-2750.
2. D. T. McQuade, A. E. Pullen and T. M. Swager, *Chemical Reviews*, 2000, **100**, 2537-2574.
3. C. Yi, W. Tian, B. Song, Y. Zheng, Z. Qi, Q. Qi and Y. Sun, *Journal of Luminescence*, 2013, **141**, 15-22.
4. L. Fabbrizzi and A. Poggi, *Chem. Soc. Rev.*, 1995, **24**, 197-202.
5. M. R. Pinto and K. S. Schanze, *Proceedings of the National Academy of Sciences of the United States of America*, 2004, **101**, 7505-7510.
6. I.-B. Kim, A. Dunkhorst, J. Gilbert and U. H. Bunz, *Macromolecules*, 2005, **38**, 4560-4562.
7. N. Singh, N. Kaur, J. Dunn, M. MacKay and J. F. Callan, *Tetrahedron Letters*, 2009, **50**, 953-956.
8. A. D. Child and J. R. Reynolds, *Macromolecules*, 1994, **27**, 1975-1977.
9. M. R. Pinto, B. M. Kristal and K. S. Schanze, *Langmuir*, 2003, **19**, 6523-6533.
10. K. K. Stokes, K. Heuzé and R. D. McCullough, *Macromolecules*, 2003, **36**, 7114-7118.
11. S. Kamila, J. F. Callan, R. C. Mulrooney and M. Middleton, *Tetrahedron Letters*, 2007, **48**, 7756-7760.
12. I.-B. Kim, J. N. Wilson and U. H. Bunz, *Chemical Communications*, 2005, 1273-1275.
13. C. Xue, V. R. Donuru and H. Liu, *Macromolecules*, 2006, **39**, 5747-5752.
14. P. B. Balanda, M. B. Ramey and J. R. Reynolds, *Macromolecules*, 1999, **32**, 3970-3978.
15. B. S. Gaylord, A. J. Heeger and G. C. Bazan, *Journal of the American Chemical Society*, 2003, **125**, 896-900.
16. H. Wu, F. Huang, Y. Mo, W. Yang, D. Wang, J. Peng and Y. Cao, *Advanced Materials*, 2004, **16**, 1826-1830.
17. O. Fix and K. Kowdley, *Minerva medica*, 2008, **99**, 605-617.
18. P. Aisen, M. Wessling-Resnick and E. A. Leibold, *Current opinion in chemical biology*, 1999, **3**, 200-206.

19. S. Altamura and M. U. Muckenthaler, *Journal of Alzheimer's Disease*, 2009, **16**, 879-895.
20. L. Silvestri and C. Camaschella, *Journal of cellular and molecular medicine*, 2008, **12**, 1548-1550.
21. (a)A. L. Crumbliss and J. M. Harrington, *Advances in inorganic chemistry*, 2009, **61**, 179; (b) M. S. Mitchell, D. L. Walker, J. Whelan and B. Bosnich, *Inorganic chemistry*, 1987, **26**, 396-400.
22. A. Ohashi, H. Ito, C. Kanai, H. Imura and K. Ohashi, *Talanta*, 2005, **65**, 525-530.
23. I. Juranovic, P. Breinhoelder and I. Steffan, *Journal of Analytical Atomic Spectrometry*, 2003, **18**, 54-58.
24. P. Ugo, L. Moretto, A. De Boni, P. Scopece and G. Mazzocchin, *Analytica chimica acta*, 2002, **474**, 147-160.
25. E. Bakkaus, R. N. Collins, J.-L. Morel and B. Gouget, *Journal of Chromatography A*, 2006, **1129**, 208-215.
26. C. M. van den Berg, *Analytical chemistry*, 2006, **78**, 156-163.
27. L. Tarazi, N. Narayanan, J. Sowell, G. Patonay and L. Strekowski, *Spectrochimica Acta Part A: Molecular and Biomolecular Spectroscopy*, 2002, **58**, 257-264.
28. J. Mao, L. Wang, W. Dou, X. Tang, Y. Yan and W. Liu, *Organic letters*, 2007, **9**, 4567-4570.
29. S. Ghosh, R. Chakrabarty and P. S. Mukherjee, *Inorganic chemistry*, 2008, **48**, 549-556.
30. A. J. Weerasinghe, C. Schmiesing, S. Varaganti, G. Ramakrishna and E. Sinn, *The Journal of Physical Chemistry B*, 2010, **114**, 9413-9419.
31. L.-F. Zhang, J.-L. Zhao, X. Zeng, L. Mu, X.-K. Jiang, M. Deng, J.-X. Zhang and G. Wei, *Sensors and Actuators B: Chemical*, 2011, **160**, 662-669.
32. B. Ma, S. Wu and F. Zeng, *Sensors and Actuators B: Chemical*, 2010, **145**, 451-456.
33. S.-R. Liu and S.-P. Wu, *Sensors and Actuators B: Chemical*, 2012, **171**, 1110-1116.
34. Q. Meng, W. Su, C. He and C. Duan, *Talanta*, 2012, **97**, 456-461.
35. V. Bravo, S. Gil, A. M. Costero, M. N. Kneeteman, U. Llaosa, P. M. Mancini, L. E. Ochando and M. Parra, *Tetrahedron*, 2012, **68**, 4882-4887.
36. Y. R. Bhorge, H.-T. Tsai, K.-F. Huang, A. J. Pape, S. N. Janaki and Y.-P. Yen, *Spectrochimica Acta Part A: Molecular and Biomolecular Spectroscopy*, 2014, **130**, 7-12.
37. C. Queirós, A. M. Silva, S. C. Lopes, G. Ivanova, P. Gameiro and M. Rangel, *Dyes and Pigments*, 2012, **93**, 1447-1455.

38. D. Staneva, P. Bosch and I. Grabchev, *Journal of Molecular Structure*, 2012, **1015**, 1-5.
39. N. R. Chereddy, M. V. N. Raju, P. Nagaraju, V. R. Krishnaswamy, P.S. Korrapati, P. R. Bangal and V. J. Rao, *Analyst*, 2014, **139**, 6352-6356.
40. D. Shi,M. Ni, J. Luo, M. Akashi, X. Liu and M. Chen, *Analyst*, 2015, **140**, 1306-1313.
41. H. Xu, S. Zhou, L. Xiao, H. Wang, S. Li and Q. Yuan, *Journal of Materials Chemistry C*, 2015, **3**, 291-297.
42. R. R. Koner, S. Sinha, S. Kumar, C. K. Nandi and S. Ghosh, *Tetrahedron Letters*, 2012, **53**, 2302-2307.
43. A. Kamal, N. Kumar, V. Bhalla, M. Kumar and R. K. Mahajan, *Sensors and Actuators B: Chemical*, 2014, **190**, 127-133.
44. Z.-Q. Liang, C.-X. Wang, J.-X. Yang, H.-W. Gao, Y.-P. Tian, X.-T. Tao and M.-H. Jiang, *New Journal of Chemistry*, 2007, **31**, 906-910.
45. M. Chhibber, G. Kumar, P. Parasuraman, T. Ramya, N. Surolia and A. Surolia, *Bioorganic & medicinal chemistry*, 2006, **14**, 8086-8098.
46. P. Goswami and D. K. Das, *Journal of Fluorescence*, 2012, **22**, 1081-1085.
47. J.-Q. Wang, L. Huang, M. Xue, Y. Wang, L. Gao, J. H. Zhu and Z. Zou, *The Journal of Physical Chemistry C*, 2008, **112**, 5014-5022.
48. A. Senthilvelan, I. Ho, K. C. Chang, G. H. Lee, Y. H. Liu and W. S. Chung, *Chemistry-A European Journal*, 2009, **15**, 6152-6160.
49. D. Schaming, C. Costa-Coquelard, I. Lampre, S. Sorgues, M. Erard, X. Liu, J. Liu, L. Sun, J. Canny and R. Thouvenot, *Inorganica Chimica Acta*, 2010, **363**, 2185-2192.
50. A. D. Becke, *The Journal of Chemical Physics*, 1993, **98**, 5648-5652.
51. C. Lee, W. Yang and R. G. Parr, *Physical Review B*, 1988, **37**, 785.
52. P. J. Hay and W. R. Wadt, *The Journal of Chemical Physics*, 1985, **82**, 270-283.
53. F. Wang, R. Nandhakumar, J. H. Moon, K. M. Kim, J. Y. Lee and J. Yoon, *Inorganic chemistry*, 2011, **50**, 2240-2245.